INDERSCIENCE PUBLISHERS
Linking academia, business and industry through research

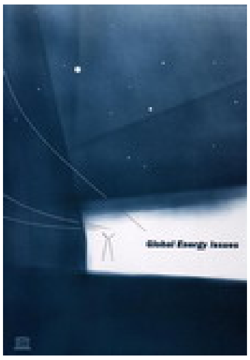

International Journal of Global Energy Issues

ISSN online: 1741-5128 - ISSN print: 0954-7118
https://www.inderscience.com/ijgei

Enhancing design efficiency of intelligent garden space allocation: an adaptive layout algorithm by multi-objective ant colony optimisation

Bo Chen, Jun Ma

DOI: 10.1504/IJGEI.2026.10077764

Article History:

Received:	30 December 2025
Last revised:	24 January 2026
Accepted:	17 February 2026
Published online:	29 April 2026

Enhancing design efficiency of intelligent garden space allocation: an adaptive layout algorithm by multi-objective ant colony optimisation

Bo Chen*

Shaanxi Fashion Engineering University,
Xi'an 712046, China
Email: 17782715550@163.com
*Corresponding author

Jun Ma

Shaanxi Boyi Construction Engineering Co., Ltd.,
Xi'an 712046, China
Email: majunj2025@163.com

Abstract: In complex urban environments, the design of urban gardens increasingly faces the challenge of balancing spatial efficiency, ecological function, and diverse human behavioural patterns. To address multi-objective optimisation scenarios, this study uses publicly available datasets: OpenStreetMap and GeoLife trajectory data. These datasets help extract urban garden structures and real-world human activity trajectories. Together, they form the basis for constructing spatial scenes and modelling behavioural constraints. Building on the classical Ant Colony Optimisation (ACO) framework, a multi-objective Pareto-front guidance mechanism is introduced to adaptively steer the search process. From a methodological perspective, this study proposes a dynamic heuristic function to enhance the algorithm's ability to address complex layout goals, including path connectivity, functional zoning diversity, and visual aesthetic harmony. This approach enables the algorithm to respond simultaneously to static spatial structures and dynamic behavioural patterns, achieving a synergistic optimisation between spatial layout and user needs.

Keywords: garden space optimisation; multi-objective ant colony algorithm; behaviour response modelling; adaptive heuristic mechanism; intelligent spatial layout.

Reference to this paper should be made as follows: Chen, B. and Ma, J. (2026) 'Enhancing design efficiency of intelligent garden space allocation: an adaptive layout algorithm by multi-objective ant colony optimisation', *Int. J. Global Energy Issues*, Vol. 48, No. 8, pp.43–62.

Biographical notes: Bo Chen obtained his bachelor's degree in Design from the School of Art and Design, Northwest University, and his master's degree in Landscape Architecture from the School of Architecture, Chang'an University. He started working in 2017 and currently serves as a teacher at the School of Art and Design, Shaanxi Fashion Engineering University. He has a solid academic foundation and rich practical experience in art design and landscape architecture, along with professional competence in design practice and teaching.

Jun Ma graduated from the School of Arts and Design at Northwest University in 2012 with a bachelor's degree in Design. In the same year, he started working at Shaanxi Boyi Construction Engineering Co., Ltd., and is now the Design Director. He is mainly responsible for overall project design planning and execution, design team management, and cross-department coordination, possessing a solid professional background in art and design and extensive practical experience in the construction engineering field.

1 Introduction

Urban gardens are a key part of urban green infrastructure. They provide essential environmental functions, including ecological regulation and biodiversity conservation. In addition, they support daily activities, promote public health, and facilitate social interaction (Awadallah et al., 2025). With accelerating urbanisation, their function has evolved from serving as mere 'visual landscapes' to becoming 'behavioural carriers', making spatial structure an increasingly critical factor in user efficiency and experience quality (Tian et al., 2023). In the context of smart cities and data-driven design, optimising garden layouts has become a key topic in urban spatial research and landscape design (Zhang and Shao, 2025). This optimisation uses spatial and behavioural data to improve the scientific basis and adaptability of functional configurations. Recent advancements in urban sensing and trajectory tracking technologies offer new opportunities for understanding user behaviour patterns and provide a solid data foundation and algorithmic support for spatial optimisation (Dorrah and Marzouk, 2021).

However, despite the increasing number and coverage of urban gardens, challenges persist in terms of spatial layout efficiency and behavioural adaptability. Traditional design approaches often rely heavily on subjective judgment, making it difficult to systematically quantify the relationships between functional zoning and behavioural responses (Wang et al., 2025). Moreover, many existing optimisation models prioritise visual aesthetics or connectivity while overlooking the dynamic nature of user behaviour and the complexity of spatial configurations. As a result, issues such as low space utilisation, inefficient pathway design, and unbalanced use of functional zones are common (Srinivasan and Venkatesan, 2021). Furthermore, most models rely on single-objective or static optimisation, lacking the capacity to address spatial diversity and user preference variability simultaneously – limiting their application in complex, real-world urban garden environments (Fathollahi-Fard et al., 2023).

In this study, behavioural adaptability refers to the ability of the layout to adjust the allocation of functional areas and the organisation of paths based on movement and dwell patterns inferred from user trajectory data. Aesthetic balance is defined as the spatial uniformity of functional area distribution and serves as a quantitative measure of visual order at the layout scale. User efficiency denotes the extent to which users can effectively access and utilise functional areas within the garden, measured by path connectivity and the average travel distance between activity nodes.

To address these challenges, this study proposes a data-driven Multi-Objective Adaptive Ant Colony Optimisation (MO-ACO). The approach aims to generate layout solutions that are structurally sound, behaviourally responsive, and aesthetically balanced in actual urban garden contexts. Leveraging open urban datasets and trajectory-based behavioural data, the method constructs a spatial graph model and a human behaviour response model. By incorporating dynamic heuristic functions and a Pareto-dominance-based multi-objective search strategy, the algorithm enables more effective alignment between spatial structure and user needs. Compared to traditional optimisation methods, MO-ACO not only improves solution diversity and convergence performance but also significantly enhances the identification of high-dwell areas and key pedestrian routes.

The contributions of this study are threefold: (1) establish a behaviour–space coupled modelling framework that integrates human preferences inferred from trajectories into spatial layout optimisation, enabling behaviour-aware design decisions; (2) develop a MO-ACO method with dynamic heuristic adjustments, allowing the optimisation process to respond to spatial attributes and behavioural feedback; and (3) validate the proposed framework using real-world OpenStreetMap and GeoLife trajectory data, demonstrating its effectiveness across various spatial structure scenarios.

2 Literature review

In summary, although significant progress has been made in model representation and algorithmic design, current approaches remain inadequate in addressing dynamic behavioural features and developing responsive layout systems. The absence of behaviour-informed adaptive optimisation mechanisms remains a major limitation in their practical implementation. Overall, to date, no studies have directly embedded adaptive behaviour modelling into the multi-objective landscape layout optimisation loop, where behavioural feedback dynamically influences the search process itself.

Early research on garden and urban green space optimisation primarily focused on spatial structure or ecological efficiency, without explicitly incorporating human behaviour into the optimisation process. As expectations for urban living environments have increased, the design of garden spaces has gradually shifted from an emphasis on formal aesthetics toward balancing structural efficiency and behavioural adaptability (Wei et al., 2022). In this context, spatial optimisation is increasingly recognised as a complex problem involving resource allocation efficiency, path organisation logic, and the compatibility between users and space. Sun et al. emphasised that effective garden design should integrate natural elements with human flow patterns to achieve a synergistic effect between ecological value and social utility (Sun et al., 2022). From an evaluation perspective, several representative metrics – such as space utilisation, path connectivity, and landscape balance – have been proposed to support the construction of objective functions in layout optimisation models (Airlangga et al., 2024; Hamzei et al., 2023).

Another line of research incorporates human behavioural information, such as survey data or trajectory statistics, into spatial planning. However, these studies typically treat behavioural factors as static inputs rather than adaptive components. In recent years, spatial optimisation has entered a model-driven stage centred on search techniques, with swarm intelligence algorithms becoming mainstream solutions (Priyadarshi and Kumar, 2025). For example, Li et al. (2023) applied Ant Colony Optimisation (ACO) to ecological corridor path planning, while Kumar et al. (2025) employed genetic algorithms to improve the balance and accessibility of park functional areas. Although these methods utilise graph-based spatial representations and multi-objective search strategies, behavioural data are usually applied only for offline evaluation or parameter calibration and do not dynamically influence the optimisation path.

More recent studies have explored data-driven or behaviour-aware spatial design, particularly through the integration of human mobility data and trajectory analysis. Tarabon et al. (2022) used mobility-based indicators to guide urban green space allocation, showing improved alignment between spatial layout and actual usage patterns. Liu et al. (2025) similarly employed mobility-informed metrics to enhance the correspondence between layout and real-world use. Yang et al. (2025) incorporated GPS trajectory density into park planning to promote activity-oriented design outcomes. Li et al. (2022) further applied human activity data to study multi-objective optimisation in public open spaces. While these studies represent important advances in behaviour-aware design, the behavioural models remain largely decoupled from the optimisation loop and remain static throughout the search process. The optimisation algorithms themselves cannot respond to continuously changing behavioural feedback.

In summary, despite significant progress in spatial modelling and algorithmic design, existing approaches remain limited in capturing dynamic behavioural characteristics and developing responsive layout systems. In particular, no prior work has directly embedded adaptive behaviour modelling into a multi-objective optimisation loop such that behavioural feedback dynamically influences the search process itself. This unresolved challenge motivates the proposed MO-ACO framework, which integrates behaviour-derived preference signals into the heuristic update mechanism, thereby enabling a weakly coupled yet adaptive interaction between human behaviour and spatial optimisation.

3 Materials and methods

The overall workflow of the proposed method follows a structured process: spatial and behavioural data collection, graph-based spatial modelling, behaviour-aware multi-objective optimisation, and layout generation. OpenStreetMap data are used to construct the spatial graph, while GeoLife trajectories provide behavioural preference signals. The MO-ACO algorithm integrates these two components to generate adaptive layout solutions.

Figure 1 illustrates the framework that integrates spatial data, behavioural modelling, and MO-ACO to generate garden layout solutions with behaviour-aware capabilities.

Figure 1 Overall framework of the proposed MO-ACO-based landscape layout optimisation (see online version for colours)

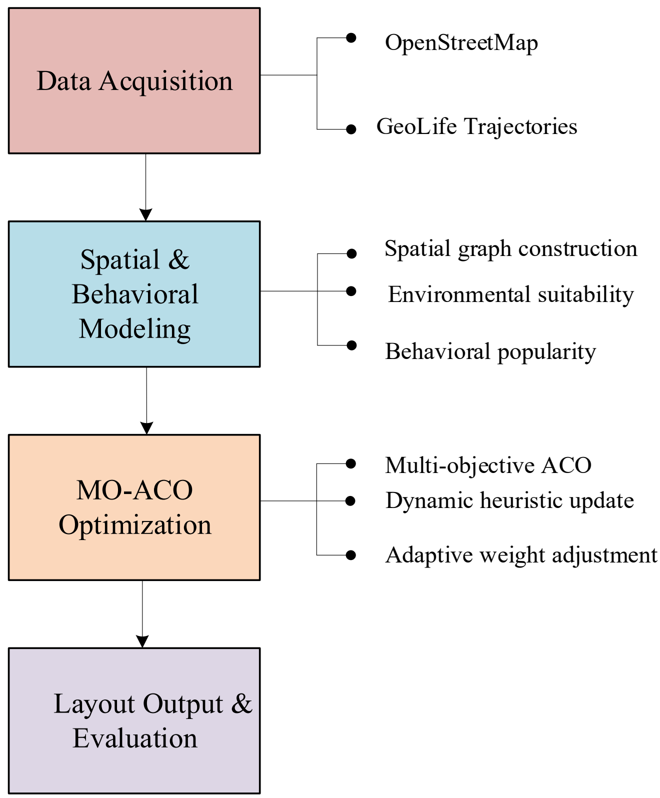

3.1 Data sources and pre-processing

This study utilises two publicly available datasets as the foundation for model construction and experimentation: one for modelling garden spatial structure and the other for capturing human behavioural responses. Spatial structure data are sourced from OpenStreetMap (OSM), while behavioural data are based on the GeoLife GPS trajectory dataset released by Microsoft Research Asia.

The OSM data were extracted using the OSMnx library (version 1.3) to identify garden boundaries within selected urban areas. Tags such as ‘leisure=park’, ‘landuse=grass’, and ‘natural=tree’ were used to filter public green spaces, functional zone boundaries, and primary path structures. The extracted data were standardised using GeoPandas and spatially modelled as polygons via Shapely. To meet the structural requirements of layout simulation, all garden areas were converted into topological graph structures, where nodes represent functional unit centres and edges denote path connectivity (Sicuaio et al., 2024; Pitakaso et al., 2024). Redundant spatial regions were normalised, and fragmented green patches were removed to enhance modelling efficiency.

The GeoLife dataset comprises GPS trajectory data from 182 users in Beijing, recorded at intervals of 1 to 5 seconds with a spatial accuracy of 5–10 metres. For behavioural model construction, all trajectories were segmented into daily time windows (6:00–22:00), and only segments located within park boundaries were retained. Two key behavioural features were extracted: (1) Path density, calculated by analysing the frequency of overlapping trajectories to generate a heatmap of path usage; and (2) Dwell hotspots, identified by clustering spatial points where dwell time exceeded 10 minutes, representing zones of high user activity.

3.2 Spatial graph construction and attribute derivation

To construct a garden layout environment suitable for adaptive optimisation, urban garden areas are modelled as a weighted undirected graph $G = (V, E)$, where the node set V represents candidate locations for functional units, and the edge set E denotes potential connection paths or line-of-sight accessibility between nodes (Şenaras et al., 2025).

Each node $v_i \in V$ is associated with an attribute vector $a_i = [s_i, c_i, h_i, l_i]$, where: s_i indicates the available deployable area at the location, c_i represents the set of candidate functional categories for the site, h_i denotes the weight of human activity intensity (behavioural heat), l_i reflects the composite suitability score derived from terrain and environmental factors. Each edge $e_{ij} \in E$ is assigned a path length d_{ij} and a connectivity priority score γ_{ij}, the latter of which is dynamically determined based on the density of paths and visual accessibility between the two nodes.

To explicitly associate human trajectory data with the spatial graph representation, trajectory-derived metrics are mapped to graph nodes to compute a behavioural popularity weight h_i for each node v_i. Specifically, the visit frequency f_i and dwell intensity d_i extracted from the GeoLife trajectories are spatially aggregated to the nearest functional node based on the Euclidean distance within the park boundary. The behavioural popularity weight is then defined as a normalised composite score:

$$h_i = \omega_1 \cdot \tilde{f}_i + \omega_2 \cdot \tilde{d}_i \tag{1}$$

where $\tilde{f}_i$ and $\tilde{d}_i$ represent the normalised visit frequency and dwell intensity, respectively, and $\omega_1 + \omega_2 = 1$. This mapping ensures that human activity patterns extracted from the raw trajectories are explicitly embedded into the spatial graph structure.

Functional zoning is defined according to common requirements in urban parks, consisting of five primary spatial unit types: rest and recreation zones, landscape exhibition zones, pedestrian pathways, water bodies/nature conservation zones, and public service facility areas. Each functional zone is classified into a type label set $C = \{c_1, c_2, ..., c_k\}$, with each type corresponding to a set of functional matching constraints and spatial layout requirements. For instance, recreational areas should be prioritised near high-dwell heat zones, while service facilities must be adjacent to primary paths or entrances (Hesarkazzazi et al., 2022).

Initial layout constraints include three aspects: (1) Spatial suitability constraint – A node is eligible only if $s_i \geq s_{\min}$; (2) Functional compatibility constraint – The candidate function c_i of a node must include the target function type. (3) Behavioural preference constraint – A weight function $w_i = \alpha h_i + \beta l_i$ is introduced as part of the heuristic in the optimisation process, where α and β are empirically defined coefficients that balance human behaviour response and environmental suitability.

The environmental suitability score l_i reflects the intrinsic spatial and environmental conditions of each candidate location and is derived from spatial features based on OpenStreetMap. Due to the lack of fine-grained environmental sensing data, l_i is constructed as a proxy indicator by integrating multiple spatial attributes that can be directly obtained from OSM. These attributes include: (1) accessibility to primary paths, measured by the shortest network distance to major pedestrian routes; (2) green space continuity, quantified by the adjacency of green polygons surrounding the node; and (3) environmental context proxies, such as proximity to water bodies or tree-covered areas inferred from OSM tags. Each attribute is normalised to the range [0,1], and the environmental suitability score is computed as a weighted sum:

$$l_i = \sum_{m=1}^{M} \theta_m \cdot \tilde{e}_{im} \tag{2}$$

where $\tilde{e}_{im}$ denotes the normalised value of the m-th environmental attribute for node v_i, θ_m is the corresponding weight, and $\sum \theta_m = 1$.

3.3 *Trajectory-based behavioural feature extraction and mapping*

The behavioural response model is constructed around three components: visit frequency distribution, path preference patterns, and dwell hotspot identification.

Visit frequency is calculated based on the number of trajectory segments covering a given spatial area (Tong et al., 2024). For each node v_i, its visit frequency f_i is computed as shown in equation (3):

$$f_i = \frac{1}{T} \sum_{t=1}^{T} \mathbb{I}\left(v_i \in \mathcal{P}_t\right) \tag{3}$$

Let $\mathcal{P}_t$ denote the sequence of nodes traversed in the t-th trajectory, $\mathbb{I}$ be an indicator function, and T the total number of trajectories. This value is used to measure the activity intensity within a spatial region, indirectly reflecting users' preferences for different functional zones.

Next, path preference patterns are derived by analysing frequently observed path sequences in the trajectory data (Salimian et al., 2022). A frequency-weighted transition probability matrix P is constructed, where the element p_{ij} represents the relative probability of a path forming from node v_i to node v_j in historical trajectories, as defined in equation (4):

$$p_{ij} = \frac{n_{ij}}{\sum_{k \neq i} n_{ik}} \tag{4}$$

n_{ij} is the number of times a trajectory transitions from v_i to v_j. This matrix is employed during the optimisation process to refine the evaluation of path accessibility, thereby ensuring that the layout aligns more closely with natural movement patterns.

Dwell hotspot identification is based on the analysis of stopping durations at specific trajectory points (Sahu et al., 2025). For each location, a dwell time threshold τ is set. If the dwell time t_i at a given node satisfies $t_i \geq \tau$, the node is marked as a high-dwell area. A dwell factor d_i is then calculated to represent the average dwell intensity at that location.

The three types of behavioural factors – visit frequency, transition probability, and dwell intensity – are normalised and integrated into a behavioural preference function, defined as follows:

$$b_i = \lambda_1 \cdot \tilde{f}_i + \lambda_2 \cdot \tilde{d}_i \tag{5}$$

where $\tilde{f}_i$ and $\tilde{d}_i$ are the normalised visit frequency and dwell factor, respectively. The coefficients λ_1, $\lambda_2 \in [0,1]$ are weighting parameters that satisfy $\lambda_1+\lambda_2=1$, and can be flexibly adjusted according to the type of functional zone.

In the behaviour-guided layout optimisation process, the behavioural preference function b_i is incorporated into the heuristic update mechanism of the ACO algorithm. It influences the probability of an ant transitioning from one state to another (Arshad et al., 2025), as shown in equation (6):

$$\eta_{ij}^{'} = \eta_{ij} \cdot \left(1 + \delta \cdot \frac{b_j}{max(b)}\right) \tag{6}$$

where $\eta_{ij}^{'}$ represents the adjusted heuristic value, and δ is the behavioural response adjustment coefficient. Through this mechanism, the system can adaptively adjust the preference direction during the layout search process, thereby enabling a shift from static structural optimisation to behaviour-driven dynamic guidance.

This study does not assume human mobility patterns are independent of spatial design. On the contrary, the extracted behavioural indicators – such as visit frequency, path transition probabilities, and dwell intensity – are incorporated as preference signals into the optimisation process, forming a weakly coupled responsive model. Within this framework, the observed trajectories provide prior behavioural tendencies that dynamically influence the layout search, rather than representing fixed or design-invariant movement patterns. This approach enables the optimisation process to remain responsive to human behaviour while avoiding strong assumptions about deterministic behaviour–design causality.

3.4 Definition of multi-objective functions and Pareto strategy

Spatial utilisation evaluates how effectively functional units are allocated within the usable layout area (Ding et al., 2025). Let $V_s \subseteq V$ represent the set of nodes selected for deployment. The objective function for spatial utilisation is defined in equation (7):

$$f_1 = \frac{\sum_{v_i \in V_s} s_i}{\sum_{v_i \in V} s_i} \tag{7}$$

where s_i denotes the deployable area associated with node v_i. This metric reflects the compactness and efficiency of the layout under the imposed constraints.

Path connectivity evaluates the accessibility and efficiency of routes between functional nodes (Rahimi et al., 2023). Let d be the average length of the weighted shortest paths between all pairs of nodes in the selected set. The objective function for connectivity is expressed as the reciprocal of the average shortest path, as shown in equation (8):

$$f_2 = \frac{1}{|V_s|\left(|V_s| - 1\right)} \sum_{v_i, v_j \in V_s, i \neq j} \frac{1}{d_{ij}} \tag{8}$$

d_{ij} denotes the path length between nodes v_i and v_j, and it is updated using weights based on the behavioural preference probability p_{ij}. This metric encourages the formation of efficient path connections between functional units.

Aesthetic balance is quantified by representing the spatial proportion of each functional zone as r_c, and using the standard deviation σ_r to measure the unevenness of functional distribution. The aesthetic objective is defined as its relative balance: $f_3 = 1 - \frac{\sigma_r}{\sigma_{max}}$, where σ_{max} denotes the theoretical maximum standard deviation. This objective is designed to promote visual and spatial harmony among functional zones, discouraging excessive clustering or large unassigned areas.

The aesthetic balance objective f_3, serving as a metric for visual balance, emphasises the spatial uniformity of functional area distribution rather than providing a comprehensive assessment of landscape aesthetics. This design approach enables the optimisation process to remain efficient while capturing the essential elements of visual order in large-scale layout designs.

Given the non-convexity and conflict among the three optimisation objectives in practical design scenarios, this study employs a non-dominated sorting strategy to construct the Pareto front solution set (Pan et al., 2021). For any two solutions x and y in the solution space, if $\forall i, f_i(x) \geq f_i(y)$ and $\exists j, f_j(x) > f_j(y)$, then x is said to dominate y. All solutions are ranked into non-dominated layers, and solution diversity is maintained through crowding distance calculation. The selection strategy is defined as: Select(x)=Rank(x)+ϵ CrowdingDistance(x), where Rank(x) denotes the non-dominated rank of solution x, CrowdingDistance(x) measures the sparsity of x in the local solution space, and ϵ is a tuning parameter.

Ultimately, by preserving a high-quality Pareto solution set throughout the multi-objective optimisation process, decision-makers are able to select the most suitable layout solution from multiple non-dominated alternatives in the output phase.

3.5 MO-ACO framework with dynamic heuristic and adaptive weights

Building upon the classical ACO algorithm, this study proposes a multi-objective optimisation framework for adaptive spatial layout in landscape design. The framework incorporates a dynamic heuristic mechanism and an adaptive weight adjustment strategy to improve search efficiency and maintain solution diversity (Nagalakshmi and Subramanian, 2024; Wang et al., 2024).

The algorithm uses a landscape graph model $G = (V, E)$ as the search space. Each ant constructs a complete layout scheme S, with the path formed by sequentially selecting functional nodes. The probability of selecting node v_j at each step is given by:

$$P_{ij} = \frac{\tau_{ij}^{\alpha} \cdot \eta_{ij}^{\beta}}{\sum_{k \in \mathcal{N}_i} \tau_{ik}^{\alpha} \cdot \eta_{ik}^{\beta}} \tag{9}$$

where τ_{ij} is the pheromone concentration, η_{ij} is the heuristic function value, α and β control their relative influence, and $\mathcal{N}_i$ is the set of candidate neighbouring nodes.

The pheromone update follows a global strategy, defined as:

$$\tau_{ij} \leftarrow (1-\rho)\tau_{ij} + \sum_{s \in \mathcal{S}^*} \Delta\tau_{ij}^{(s)} \tag{10}$$

where ρ is the pheromone evaporation rate, $\mathcal{S}^*$ denotes the current set of non-dominated Pareto solutions, and $\Delta\tau_{ij}^{(s)}$ is proportionally distributed based on the quality of each solution.

To enhance goal-directed behaviour, a dynamic heuristic function is introduced, which adjusts in real time according to node behavioural factors and spatial attributes (Dhiman and Alghamdi, 2024):

$$\eta_{ij}^{'} = \eta_{ij} \cdot \left(1 + \delta \cdot \frac{b_j}{max(b)}\right) \tag{11}$$

where b_j is the behavioural preference score, and δ controls the strength of the adjustment. This mechanism steers the search toward areas of high visitation frequency and prolonged dwell times, enhancing the behavioural responsiveness of the resulting layout. For the ablation analysis, this study reports a static behavioural variant, in which the formulation follows equation (12) and δ remains constant across all iterations. This setup allows the effect of behavioural information to be distinguished from that of the dynamic heuristic adjustment.

To reflect the varying importance of objectives at different optimisation stages, the algorithm applies dynamic objective weights, defined by:

$$w_k(t) = w_k(0) + \mu \cdot \frac{\partial f_k}{\partial t} \tag{12}$$

where $w_k(t)$ is the weight of the k-th objective at iteration t, μ is a regulation factor, and $\frac{\partial f_k}{\partial t}$ represents the recent rate of improvement of the k-th objective. Objectives showing faster convergence receive relatively less attention, promoting a more balanced optimisation process.

The use of $\frac{\partial f_k}{\partial t}$ is conceptually derived from gradient-based optimisation but does not represent an actual analytic gradient. Instead, it serves as a heuristic indicator to reflect the recent improvement trend of each objective function, guiding the adaptive weight adjustment in the swarm intelligence-based search process.

The proposed MO-ACO algorithm involves several hyperparameters, including α, β, ρ, δ, μ, and the behavioural preference weights λ_1 and λ_2. These parameters are not set arbitrarily. Their initial ranges are determined based on common settings in swarm intelligence-based spatial optimisation studies. The final values are selected through empirical tuning and grid-search experiments to ensure stable convergence and fair comparisons across algorithms.

Different functional zones adopt distinct behavioural weight configurations to reflect their varying sensitivity to human activity patterns. For example, resting areas and landscape display zones are assigned higher weights for dwell intensity, whereas pathway-oriented zones emphasise visit frequency. Once configured, these weight settings remain fixed across all comparative experiments to guarantee reproducibility and fairness.

The OpenStreetMap (OSM) data used in this study were extracted from the Beijing metropolitan area, corresponding to the administrative boundary of Beijing. Spatial data were obtained from the Geofabrik OSM repository (https://download.geofabrik.de/asia/china/beijing.html), which provides regularly updated and standardised OSM extracts. Only features relevant to public green spaces and garden environments were retained, including areas tagged as leisure=park, landuse=grass, natural=tree, and associated pedestrian paths. Small, scattered, or isolated green patches below a predefined minimum area threshold were removed to reduce spatial noise. The remaining polygons were converted into a topological graph, where nodes represent the centroids of candidate functional units, and edges represent walkable paths extracted from the OSM road and pedestrian network.

The GeoLife trajectory dataset was obtained from the official Microsoft Research repository (https://www.microsoft.com/en-us/download/details.aspx?id=52367). It contains GPS trajectories of 182 users collected in Beijing from April 2007 to October 2012, with a sampling interval of 1–5 seconds and an average spatial accuracy of approximately 5–10 metres. Trajectories were filtered to retain only records within the spatial boundaries of the selected garden areas and within the time window 06:00–22:00, corresponding to typical park usage hours. Original trajectories were segmented, and dwell events were identified using a minimum dwell time threshold of 10 minutes. Each trajectory segment was mapped to the nearest graph node or edge in the garden graph using a distance-based matching rule, enabling node-level aggregation of visit frequency, path usage, and dwell intensity.

These pre-processing steps ensure a consistent transformation from the raw spatial and trajectory data to the graph-based representation used in subsequent behavioural modelling and optimisation experiments.

4 Results and discussion

4.1 Comparative analysis of multi-model performance

To evaluate the overall performance of the proposed MO-ACO across different landscape layout scenarios, simulation experiments were conducted on three representative types of spatial structures. These structures were all derived from real-world landscape spatial data in Beijing, with variations in spatial layout patterns and connectivity characteristics. The specific types are as follows: Structure Type A (Centralised): Features a compact overall layout, with functional zones organised around a central node. It exhibits high path accessibility and is typically suitable for urban core parks. Structure Type B (Linear/Belt-shaped): Characterised by narrow and elongated green spaces, with path systems displaying linear or dendritic patterns. This type is commonly found along urban riverbanks or transportation corridors. Structure Type C (Dispersed): Functional nodes are loosely distributed and separated by terrain or buildings, resulting in weak connectivity. This structure represents peripheral, community-oriented green space networks.

For each structural type, the proposed MO-ACO method was compared against four mainstream optimisation algorithms: Traditional ACO, NSGA-II, GA, Strength Pareto Evolutionary Algorithm 2 (SPEA2) – featuring enhanced elitism, and MOEA/D. All experiments were independently run for 10 iterations. Three key performance metrics were calculated: spatial utilisation (f_1), path connectivity (f_2), and aesthetic balance (f_3). Figure 2 summarises the mean and standard deviation of each method's performance across the three structural scenarios.

Figure 2 Comparison of layout performance across three types of landscape structures using different algorithms (a: MO-ACO, ACO, NSGA-II; b: GA, SPEA2, MOEA/D) (see online version for colours)

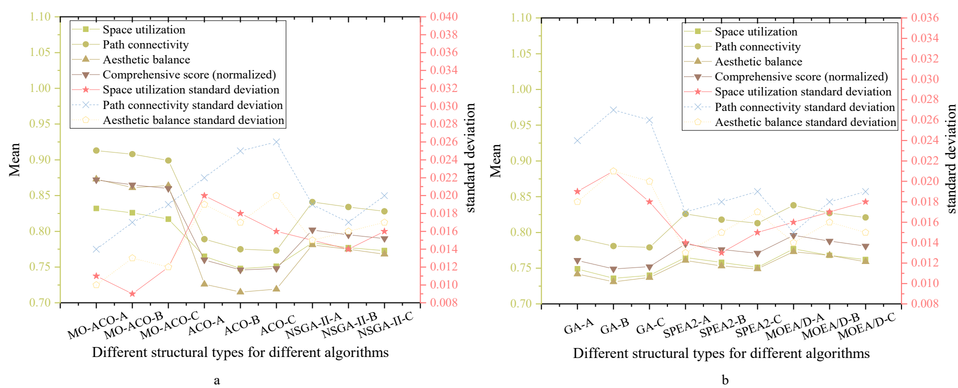

As illustrated in Figure 2, the proposed MO-ACO algorithm achieved the highest overall performance across all three structural scenarios: 0.872 for the centralised layout, 0.865 for the linear layout, and 0.860 for the dispersed layout. These results highlight MO-ACO's strong adaptability to varying spatial structures and its effectiveness in multi-objective optimisation. Notably, the algorithm delivered substantial improvements in both path connectivity and aesthetic balance. This confirms the benefits of incorporating behaviour-based preference functions and a dynamic heuristic mechanism. MOEA/D demonstrated generally stable performance, achieving slightly higher scores than NSGA-II and SPEA2. It performed particularly well in the centralised and linear layouts, with connectivity scores of 0.838 and 0.827, respectively. This suggests that its decomposition-based strategy is well suited to more regular spatial structures. However, in the dispersed layout, MOEA/D scored significantly lower on aesthetic balance (0.759) compared to MO-ACO (0.864), indicating limitations in handling complex behavioural constraints. Both NSGA-II and SPEA2 delivered moderate results across all metrics. However, they consistently underperformed relative to MO-ACO, particularly in solution diversity and spatial utilisation efficiency.

4.2 Analysis of Pareto front quality and solution distribution

To further evaluate the quality of solutions generated by each algorithm for the multi-objective layout task, performance was assessed using three established indicators:

- Hypervolume (HV): Measures the volume of the objective space dominated by the non-dominated solution set. Higher values indicate better performance.
- Generational Distance (GD): Represents the average distance from the obtained solutions to the true Pareto front. Lower values are preferred.
- Spread (Δ): Reflects the uniformity and diversity of the solution distribution. Smaller values suggest better dispersion.

Since the true theoretical Pareto front for the studied multi-objective layout problem is unknown, the reference Pareto front used for calculating the GD is constructed empirically. Specifically, it is defined as the union of all non-dominated solutions obtained by all compared algorithms across all independent runs.

These metrics were calculated based on results from the three-objective optimisation task – spatial utilisation, path connectivity, and aesthetic balance – conducted under the centralised landscape structure (Structure Type A). The reported values represent averages from 10 independent experimental runs.

Figure 3 Comparison of non-dominated solution set quality in centralised landscape structures using different algorithms (see online version for colours)

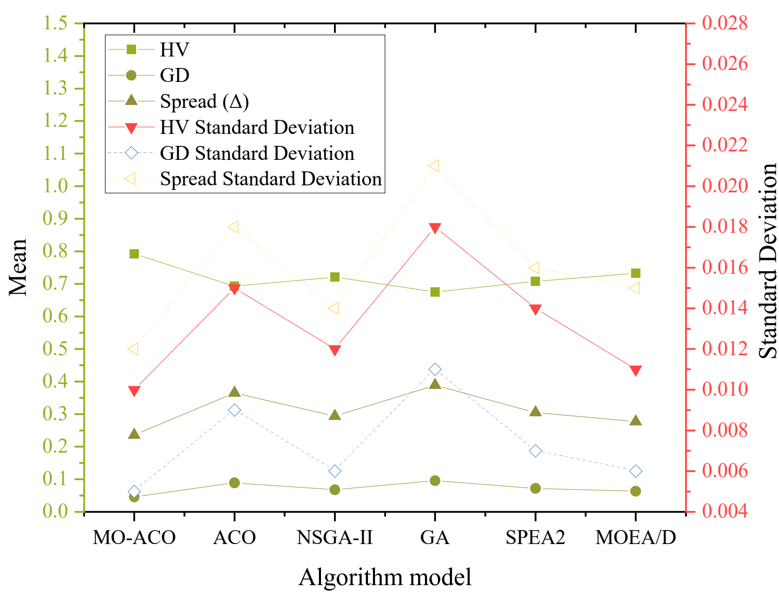

As shown in Figure 3, MO-ACO consistently outperformed all other algorithms across the three evaluation metrics. It achieved the highest Hypervolume score (0.792), significantly exceeding those of traditional ACO (0.693) and NSGA-II (0.721), indicating more comprehensive coverage of the high-quality solution space within the three-objective domain. For Generational Distance (GD), MO-ACO reported the lowest value (0.046), suggesting that its Pareto front is closest to the theoretical optimum. In contrast, GA and ACO yielded higher GD values – 0.096 and 0.089, respectively – indicating weaker convergence performance. In terms of solution diversity, MO-ACO achieved the lowest Spread value (0.236), reflecting a well-distributed set of solutions along the Pareto front. By comparison, ACO and GA had significantly higher Spread values (0.365 and 0.389), pointing to greater dispersion and a higher risk of solution clustering or skewed distributions.

4.3 Impact analysis of the dynamic heuristic mechanism

To evaluate the role of the dynamic heuristic mechanism in the optimisation process, a comparative analysis was conducted under three configurations: MO-ACO (with dynamic heuristic): The full model, incorporating behaviour-based adjustments to heuristic weights. MO-ACO (without dynamic heuristic): A simplified version using only static heuristic information, without behaviour-sensitive tuning and a control group: static behavioural weights. The experiments were conducted in a centralised landscape structure scenario and evaluated using the following key indicators: 1. Final convergence values of the three objective functions: spatial utilisation, path connectivity, and aesthetic balance. 2. Average number of iterations required to reach 95% of the optimal solution. 3. Frequency of local optima entrapment, defined as failure to improve results in at least 3 out of 10 independent runs. The detailed results of this comparison are presented in Table 1.

Table 1 Performance comparison with and without the dynamic heuristic mechanism (centralised structure scenario, mean ± standard deviation)

Algorithm version	*Space utilisation*	*Path connectivity*	*Aesthetic balance*	*Average convergence rounds*	*Number of local optimal traps*
MO-ACO (with dynamic)	0.832 ± 0.011	0.913 ± 0.014	0.873 ± 0.010	62 ± 4	0/10
MO-ACO (static behaviour weights)	0.816 ± 0.012	0.895 ± 0.015	0.852 ± 0.011	73 ± 5	1/10
MO-ACO (no dynamic)	0.799 ± 0.014	0.874 ± 0.017	0.832 ± 0.013	84 ± 6	3/10

Table 1 presents a three-factor ablation analysis to distinguish the contributions of behavioural information and dynamic heuristic adjustment. Compared with the behaviour-free baseline, incorporating static behaviour-preference weights increases f_1 from 0.799 to 0.816 (+0.017), f_2 from 0.874 to 0.895 (+0.021), and f_3 from 0.832 to 0.852 (+0.020), indicating that trajectory-derived behavioural signals provide a consistent guiding advantage. Enabling dynamic heuristic adjustment further improves f_1 to 0.832 (+0.016 over the static variant), f_2 to 0.913 (+0.018), and f_3 to 0.873 (+0.021), while reducing the average number of convergence iterations from 73 to 62 and eliminating local optima (from 1/10 to 0/10). These results demonstrate that performance gains are jointly driven by (i) behaviour-aware guidance and (ii) dynamic adaptation of the heuristic algorithm, the latter primarily contributing to faster convergence and enhanced robustness.

4.4 Behavioural modelling and spatial adaptability analysis

To assess the practical impact of behavioural modelling in the optimisation process, a comparative experiment was conducted under two conditions: with and without the behavioural modelling mechanism. The final spatial layout of the park was evaluated against real-world user activity patterns, using six key spatial matching indicators: Path Similarity Score (PSS): Measures the spatial overlap between the generated layout paths and actual user trajectories. Jaccard Index for Dwell Hotspot Overlap (JH): Quantifies the intersection-over-union between high-dwell functional zones in the layout and observed dwell hotspots from user trajectories. Preference Match Rate (PMR): Represents the proportion of frequently visited areas correctly assigned to user-preferred functional zones. Functional Misallocation Rate (FMR): Indicates the proportion of behaviourally significant hotspots that were not assigned appropriate functional types. Behavioural Drift Distance (BDD): Measures the spatial distance between the centre of functional zone allocation and the behavioural activity centre. Composite Response Index (CRI): A normalised aggregate score that combines all the above indicators, with values ranging from 0 to 1. The experiment was carried out using a centralised spatial structure scenario (Type A), and the average results across 10 independent runs are illustrated in Figure 4.

Figure 4 Comparison of spatial matching indicators with and without behavioural modelling mechanism (structure type A) (see online version for colours)

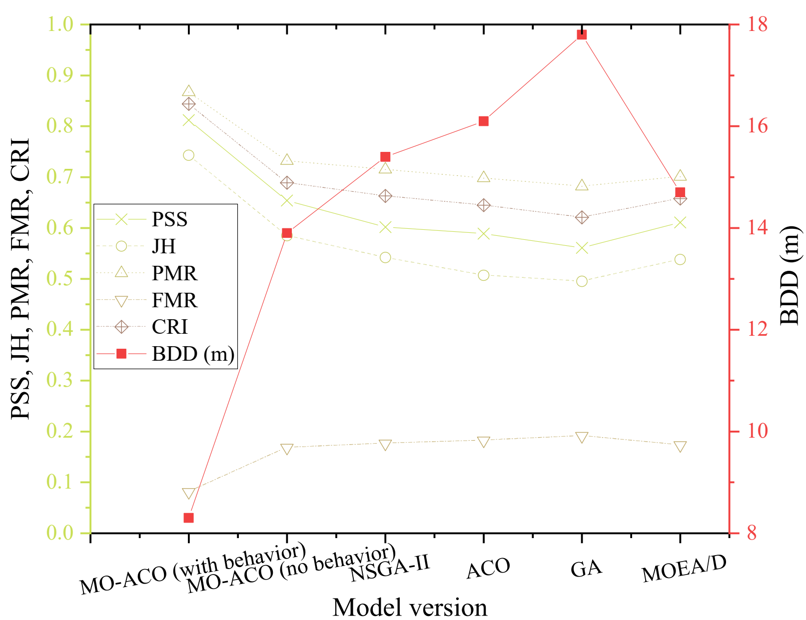

As shown in Figure 4, the MO-ACO algorithm consistently outperformed other variants across all spatial matching metrics when behavioural modelling was incorporated. The PSS increased to 0.812, significantly higher than the 0.654 achieved without behavioural modelling, indicating that the optimised path layouts more accurately reflected user movement preferences. The Jaccard Index for dwell hotspot overlap rose from 0.585 to 0.743, suggesting more accurate alignment of high-dwell areas with functional zones.

The PMR reached 0.867 – substantially higher than those of NSGA-II and GA – demonstrating improved consistency between functional allocation and user preferences. Additionally, the FMR declined markedly, showing that high-frequency behaviour areas were more appropriately assigned. The BDD was reduced from 13.9 metres to 8.3 metres, indicating a closer match between spatial layout and user activity centres. Finally, the CRI improved from 0.689 to 0.844, confirming the enhanced spatial responsiveness achieved through behavioural modelling.

4.5 Comprehensive statistical analysis and stability evaluation

To evaluate the stability and statistical significance of each optimisation algorithm across different objective functions, this section presents results from 10 independent runs. The Performance Variance Analysis assesses the consistency of algorithm outputs. The Friedman Test, a non-parametric method, determines whether overall differences among multiple algorithms are statistically significant. The Nemenyi Post-hoc Test is then used to analyse pairwise differences between algorithms. Figure 5 displays the performance variances, Friedman test results, and significance comparisons for all six algorithms across the three objective metrics.

Figure 5 Variance and statistical test results across three metrics for six algorithms (see online version for colours)

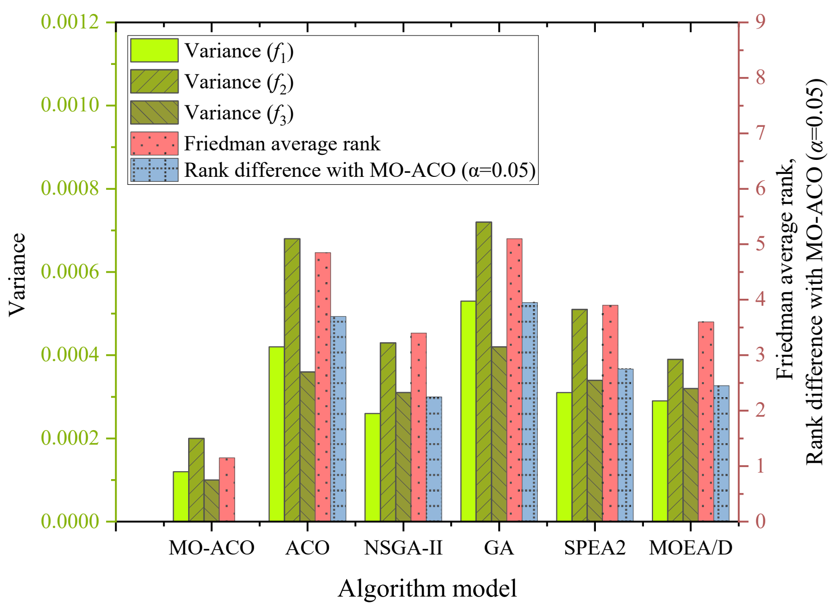

Notes: When the average rank difference exceeds the Nemenyi Critical Distance (CD, approximately 1.96 at α = 0.05, depending on the number of samples), the difference is considered statistically significant.

As illustrated in the variance results in Figure 5, MO-ACO demonstrates the lowest output variance across all three evaluation metrics (each less than 0.0002), reflecting a high degree of operational stability. In contrast, GA and ACO exhibit much higher variances, indicating that their performance is more sensitive to initialisation and search path variability – an indication of weaker robustness. The Friedman test confirms that the overall performance differences among the algorithms are statistically significant ($p < 0.01$), with MO-ACO achieving the lowest average rank (1.15), representing the best overall performance. The Nemenyi post-hoc test further supports this finding, showing that MO-ACO significantly outperforms all other algorithms at the $\alpha = 0.05$ significance level.

5 Discussion

MO-ACO consistently outperformed traditional optimisation methods across various spatial structure scenarios. Its advantage extends beyond numerical performance; it stems from a mechanism that effectively integrates both spatial structure and user behaviour characteristics. Unlike algorithms that rely solely on global search or rule-based allocation, MO-ACO dynamically adjusts heuristic weights throughout the optimisation process. This makes the search more adaptive to specific goals and more responsive to local features. Such adaptability is especially beneficial in landscape planning contexts, where spatial heterogeneity and behavioural intensity often vary significantly. The dynamic heuristic mechanism enhances convergence in the early stages by prioritising high-dwell and high-traffic areas, and it helps the algorithm avoid becoming trapped in local optima. In addition, incorporating behavioural modelling significantly improves the spatial responsiveness of the optimisation results. Traditional multi-objective algorithms often struggle to address unstructured behavioural preferences – such as movement patterns or usage density. MO-ACO addresses this challenge by converting trajectory density and dwell behaviour into heuristic guidance. This approach effectively bridges the gap between spatial resource allocation ('spatial supply') and actual user activity patterns ('behavioural demand'). As a result, the allocation of functional zones is more closely aligned with real-world usage, particularly in areas with complex structures or conflicting functional requirements, where MO-ACO demonstrates more effective distribution strategies. Furthermore, its Pareto-guided selection strategy maintains a balanced trade-off among multiple objectives, helping to preserve solution diversity and avoid bias toward any single optimisation goal. Although the aesthetic objective adopted in this study effectively reflects spatial balance, it does not explicitly capture higher-level visual perception factors such as line-of-sight continuity, colour harmony, or spatial sequence experience. These aspects are closely related to human landscape perception but require additional data sources or perceptual modelling techniques. Future research could extend the current framework by incorporating methods such as visibility graph analysis, visual corridor metrics, or image-based aesthetic evaluation to provide a more comprehensive representation of landscape aesthetics. Meanwhile, although the proposed MO-ACO framework is generally effective, certain limitations remain. In environments where behavioural data are extremely sparse, highly noisy, or biased toward specific user groups, behaviour-based heuristics may provide misleading guidance, reducing the robustness of the optimisation. Moreover, strong behavioural preferences may sometimes conflict with ecological or environmental objectives, such as biodiversity conservation or habitat connectivity. In such cases, the multi-objective framework does not enforce predefined priorities but instead reveals trade-offs through the Pareto-optimal solution set. Future research could explore the incorporation of reliability-weighted behaviour, uncertainty modelling, or the integration of ecological constraints to improve decision support under conflicting objectives or data-scarce scenarios.

6 Conclusions

This study presents a MO-ACO algorithm designed for optimising landscape spatial layouts. The approach integrates spatial data from OSM with behavioural data from GeoLife to build a spatial graph model and a corresponding human behaviour response model. By combining a dynamic heuristic mechanism with a Pareto front-driven optimisation strategy, MO-ACO facilitates the joint optimisation of spatial structure and user behaviour preferences. Experimental results across various representative spatial configurations show that MO-ACO consistently outperforms conventional algorithms – such as standard ACO, NSGA-II, and MOEA/D – on key performance indicators including spatial utilisation, path connectivity, and aesthetic balance. Moreover, MO-ACO generates higher-quality solution sets with improved responsiveness to spatial needs. The integration of behaviour modelling further enhances alignment between the optimised layout and actual user activity patterns. The algorithm more accurately captures path preferences, dwell hotspots, and functional zone allocations, confirming the effectiveness of its behaviour-aware mechanism. Despite these advantages, the study has several limitations. First, the trajectory data is restricted to urban areas of Beijing, which limits the geographic diversity of the test scenarios and reduces the potential for broader generalisation. Second, the current behaviour model does not incorporate group dynamics or temporal variations, making it less capable of reflecting differing spatial preferences across user types and times of day. Future research will focus on expanding the algorithm's application to multi-city and multi-scale environments, incorporating dynamic pedestrian flow simulations and diverse user behaviour models. These improvements aim to enhance the model's generalisability and practical utility, paving the way for deployment in real-world intelligent spatial design applications – particularly in areas such as urban public space planning and ecological restoration.

Declaration

All authors declare that they have no conflicts of interest.

References

Airlangga, G., Sukwadi, R., Basuki, W.W., Sugianto, L.F., Nugroho, O.I., Kristian, Y., et al. (2024) 'Adaptive path planning for multi-UAV systems in dynamic 3D environments: a multi-objective framework', *Designs*, Vol. 8, No. 6, 136.

Arshad, M.W., Lodi, S. and Liu, D.Q. (2025) 'Multi-objective optimization of independent automotive suspension by AI and quantum approaches: a systematic review', *Machines*, Vol. 13, No. 3, 21.

Awadallah, M.A., Makhadmeh, S.N., Al-Betar, M.A., Dalbah, L.M., Al-Redhaei, A., Kouka, S., et al. (2025) 'Multi-objective ant colony optimization', *Archives of Computational Methods in Engineering*, Vol. 32, No. 2, pp.995–1037.

Dhiman, G. and Alghamdi, N.S. (2024) 'SMOSE: Artificial intelligence-based smart city framework using multi-objective and IoT approach for consumer electronics application', *IEEE Transactions on Consumer Electronics*, Vol. 70, No. 1, pp.3848–3855.

Ding, M., Yin, X., Pan, S. and Liu, P. (2025) 'Multi-objective spatial optimization of protective forests based on the non-dominated sorting genetic algorithm II and future land use simulation model: a case study of Alaer City, China', *Forests*, Vol. 16, No. 3, 452.

Dorrah, D.H. and Marzouk, M. (2021) 'Integrated multi-objective optimization and agent-based building occupancy modeling for space layout planning', *Journal of Building Engineering*, Vol. 34, 101902.

Fathollahi-Fard, A.M., Tian, G., Ke, H., Fu, Y. and Wong, K.Y. (2023) 'Efficient multi-objective metaheuristic algorithm for sustainable harvest planning problem', *Computers & Operations Research*, Vol. 158, 106304.

Hamzei, M., Khandagh, S. and Jafari Navimipour, N. (2023) 'A quality-of-service-aware service composition method in the Internet of Things using a multi-objective fuzzy-based hybrid algorithm', *Sensors*, Vol. 23(16), 7233.

Hesarkazzazi, S., Hajibabaei, M., Bakhshipour, A.E., Dittmer, U., Haghighi, A. and Sitzenfrei, R. (2022) 'Generation of optimal (de)centralized layouts for urban drainage systems: a graph-theory-based combinatorial multi-objective optimization framework', *Sustainable Cities and Society*, Vol. 81, 103827.

Kumar, S., Tejani, G.G., Mehta, P., Sait, S.M., Yildiz, A.R. and Mirjalili, S. (2025) 'Optimization of truss structures using multi-objective cheetah optimizer', *Mechanics Based Design of Structures and Machines*, Vol. 53, No. 2, pp.1494–1515.

Li, B., Guo, T., Mei, Y., Li, Y., Chen, J., Zhang, Y., et al. (2023) 'A multi-objective memetic algorithm with adaptive local search for airspace complexity mitigation', *Swarm and Evolutionary Computation*, Vol. 83, 101400.

Li, Y., Su, S., Liu, B., Yamashita, K., Li, Y. and Du, L. (2022) 'Trajectory-driven planning of electric taxi charging stations based on cumulative prospect theory', *Sustainable Cities and Society*, Vol. 86, 104125.

Liu, Y., Kwan, M.-P., Song, L., Yu, C. and Cui, Y. (2025) 'How mobility-based exposure measures may mitigate the underestimation of the association between green space exposures and health', *Social Science & Medicine*, Vol. 336, 118190.

Nagalakshmi, B. and Subramanian, S. (2024) 'An efficient multi-objective task scheduling in edge computing using adaptive honey badger optimisation', *International Journal of Web Engineering and Technology*, Vol. 19, No. 2, pp.110–126.

Pan, T., Zhang, Y., Su, F., Lyne, V., Cheng, F. and Xiao, H. (2021) 'Practical efficient regional land-use planning using constrained multi-objective genetic algorithm optimization', *ISPRS International Journal of Geo-Information*, Vol. 10, No. 2, 100.

Pitakaso, R., Srichok, T., Khonjun, S., Gonwirat, S., Nanthasamroeng, N. and Boonmee, C. (2024) 'Multi-objective sustainability tourist trip design: an innovative approach for balancing tourists' preferences with key sustainability considerations', *Journal of Cleaner Production*, Vol. 449, 141486.

Priyadarshi, R. and Kumar, R.R. (2025) 'Evolution of swarm intelligence: a systematic review of particle swarm and ant colony optimization approaches in modern research', *Archives of Computational Methods in Engineering*, Vol. 32, pp.1–42.

Rahimi, I., Gandomi, A.H., Chen, F. and Mezura-Montes, E. (2023) 'A review on constraint handling techniques for population-based algorithms: from single-objective to multi-objective optimization', *Archives of Computational Methods in Engineering*, Vol. 30, No. 3, pp.2181–2209.

Sahu, D., Sinha, P., Prakash, S., Yang, T., Rathore, R.S. and Wang, L. (2025) 'A multi-objective optimization framework for smart parking using digital twin Pareto front MDP and PSO for smart cities', *Scientific Reports*, Vol. 15, No. 1, 7783.

Salimian, M., Ghobaei-Arani, M. and Shahidinejad, A. (2022) 'An evolutionary multi-objective optimization technique to deploy the IoT services in fog-enabled networks: an autonomous approach', *Applied Artificial Intelligence*, Vol. 36, No. 1, 2008149.

Şenaras, O.M., İnanç, Ş., Şenaras, A.E. and Öngen Bilir, B. (2025) 'Comparing the use of ant colony optimization and genetic algorithms to organize kitting systems within green supply chain management practices', *Sustainability*, Vol. 17, No. 5, 2001.

Sicuaio, T., Zhao, P., Pilesjö, P., Shindyapin, A. and Mansourian, A. (2024) 'Sustainable and resilient land use planning: A multi-objective optimization approach', *ISPRS International Journal of Geo-Information*, Vol. 13, No. 3, 99.

Srinivasan, B. and Venkatesan, R. (2021) 'Multi-objective optimization for energy- and heat-aware VLSI floorplanning using enhanced firefly optimization', *Soft Computing*, Vol. 25, No. 5, pp.4159–4174.

Sun, H., Chen, Y., Ma, J., Wang, Y., Liu, X. and Wang, J. (2022) 'Multi-objective optimal travel route recommendation for tourists by improved ant colony optimization algorithm', *Journal of Advanced Transportation*, Vol. 2022, No. 1, 6386119.

Tarabon, S., Godet, C., Coskun, T. and Clauzel, C. (2022) 'Coupling spatial modeling with expert opinion approaches to restore multispecies connectivity of major transportation infrastructure', *Landscape and Urban Planning*, Vol. 221, 104371.

Tian, H., Mo, Z., Ma, C., Xiao, J., Jia, R., Lan, Y., et al. (2023) 'Design and validation of a multi-objective waypoint planning algorithm for UAV spraying in orchards based on improved ant colony algorithm', *Frontiers in Plant Science*, Vol. 14, 1101828.

Tong, Z., Liu, Y., Zhang, Z., Pang, B., An, R., Lu, Y., et al. (2024) 'Incorporating historical information into the multi-type ant colony optimization model to optimize patch-level land use allocation', *Sustainable Cities and Society*, Vol. 106, 105404.

Wang, Q., Xu, X., Ding, X., Chen, T., Deng, R., Li, J., et al. (2024) 'Multi-objective optimization and evaluation approach of prefabricated component combination solutions using NSGA-II and simulated annealing optimized projection pursuit method',. *Scientific Reports*, Vol. 14, No. 1, 16688.

Wang, X., Sun, W., Lan, Y. and Ge, X. (2025) 'Layout optimization of low-impact development facilities based on a multi-objective genetic algorithm and the SWMM model', *Water Resources Management*, Vol. 39, pp.1–22.

Wei, F., Xu, W. and Hua, C. (2022) 'A multi-objective optimization of physical activity spaces', *Land*, Vol. 11(11), 1991.

Yang, X., Zhang, C. and Yang, L. (2025) 'Revealing spatial patterns and environmental influences on jogging volume and speed: Insights from crowd-sourced GPS trajectory data and random forest', *ISPRS International Journal of Geo-Information*, Vol. 14, No. 2, 80.

Zhang, Z. and Shao, C. (2025) 'Optimization of landscape path and facility layout in public environment design based on ant colony algorithm', *Journal of Combinatorial Mathematics and Combinatorial Computing*, Vol. 127, pp.7027–7041.